Journal of Basic and Applied Engineering Research
p-ISSN: 2350-0077; e-ISSN: 2350-0255; Volume 4, Issue 7; October-December, 2017, pp. 592-595

http://www.krishisanskriti.org/Publication.html

Synthesis of Indium Oxide Nanostructures and their Growth Mechanism

Ashaq Hussain Sofi[*1], Mohammad Ashraf Shah[2] and Kandasami Asokan[3]

[1,2]Department of Physics, NIT-Srinagar, J&K, India
[3]Material Science Division, IUAC, New Delhi, India
E-mail: [1]shifs237@gmail.com, [2]shah@nitsri.net, [3]asokaniuac@gmail.com

Abstract—*Indium oxide nanostructures were synthesized by a simple citrate gel process. The starting materials utilized were indium nitrate ($In(NO_3)_3$. xH_2O), citric acid ($C_6H_8O_7$) and de-ionized water. The role of citric acid in de-ionized water is to form metal complex in the solution i.e. it accomplishes the function of a chelating ligand. The molar ratio of the indium nitrate and citric acid were taken as 2:1 in order to avoid turbity and precipitation. The x-ray diffraction (XRD) study revealed high phase purity and crystallinity with a crystallite size of 21.25 nm. Scanning electron microscopy revealed the formation of spherical nanostructures and electron dispersive spectroscopic (EDX) analysis confirmed presence of Indium and oxygen only. Besides, synthesis and characterization the growth mechanism was also discussed in detail.*

Keywords*: Citrate gel process, Indium oxide nanostructures, Nucleation and growth.*

1. INTRODUCTION

Nanostructured materials are promising for the fabrication of novel devices as these display unusual physical properties, which differ from their bulk counter parts. In the past recent decades, a wide number of nanosized powders have been synthesized to engineer their chemical, mechanical, electrical and optical properties. It is well known from the literature that the physical properties of the nanostructures are greatly influenced by the shape, size and size-distribution at small units, which in turn are dependent on their synthesis methods [1]. Among these nanostructured materials, metal oxide semiconductors, having diverse technological applications have been under extensive research because of their high surface area, lower power consumption, high compatibility with microelectronics etc., with controlled synthesis leading to uniform shape and size [2]. The development of facile synthetic methods to synthesize nanostructures remains a challenge to scientific community in terms of cost, viable route and mass production.

Among the various metal oxides, In_2O_3 is an important n-type semiconductor with a direct energy band gap of ~ 3.6 eV. It finds impending applications in solar cells, UV-lasers, detectors, gas sensors, etc., because of its remarkable structural, electrical and the optical properties [3-5]. For these impending applications, fabrication methods played a vital role to synthesize In_2O_3 nanostructures with diverse morphology and enhanced physical as well as chemical properties. Nanostructures of In_2O_3 of diverse morphologies like lotus-root-like [6], nanorod bundles and spheres [7], and hollow microspheres [8] were synthesized by employing several synthetic routes, such as solvothermal method [7], sol-gel [9], controlled precipitation [10], forced hydrolysis [11], etc.

In the present study, In_2O_3 nanoparticles having spherical shape were synthesized by a simple citrate gel process using indium nitrate, citric acid and de-ionized water as starting materials. The study focuses on the structural and morphology features of the In_2O_3 nanostructures. Besides, synthesis and characterization the growth mechanism was also discussed in detail.

2. EXPERIMENTAL

Indium oxide (In_2O_3) nanostructures were synthesized by a simple citrate gel route. Indium nitrate [In $(NO_3).xH_2O$ (99.99%, Alpha Aesar)], citric acid [$C_6H_8O_7.H_2O$ (99.5%, Alpha Aesar)] and de-ionized water were used as starting materials to prepare the nanostructures. Two separate solutions of indium nitrate (0.4 M) and citric acid (0.8 M) were mixed and magnetically stirred at 70^0 C for one hour. The temperature of the solution was raised to 100^0 C to remove excess of water and heating was continued at the same temperature till gel is formed. The formed gel was thermally decomposed into powder at a temperature of 200 ^{0}C for 3 hours. The obtained powder was finally calcinated at a temperature of 500 ^{0}C for one hour. The schematic diagram of the synthesis process is shown in fig.1 below:

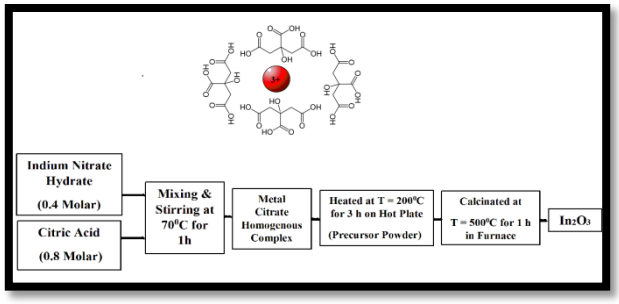

Figure 1: Schematic diagram of the synthesis process

3. RESULTS AND DISCUSSION

The crystalline structure and the phase purity of the synthesized nanostructure were studied by x-ray diffraction (XRD) measurement using Smart-lab, Rigaku Japan x-ray diffractometer (Cu Kα radiation; λ = 1.54Å) operated at 30 kV and 40 mA in the 2θ range of 10^0-80^0 with a scan speed of 1.000 deg. /min. Fig. 2 shows the XRD- pattern of In_2O_3 nanostructures in the 2θ range of 10^0-60^0. The diffraction pattern showed the BCC-structure of In_2O_3 and all the indexed peaks agreed well with the JCPDS-76-0152. No other peaks corresponding to any impurity were depicted in the pattern reflecting high phase purity of the as synthesized sample.

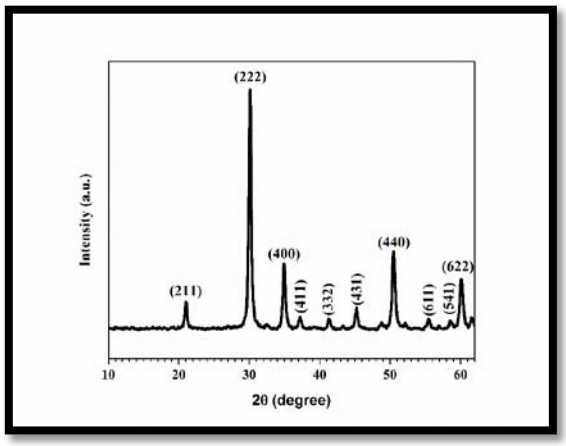

Figure 2. XRD patterns for In_2O_3 nanostructures.

The crystallite size of the synthesized samples was enumerated using the well-known Scherer's equation [12]

$$D = \frac{k\lambda}{\beta cos\theta} = \frac{0.9\lambda}{\beta cos\theta}$$

where D is the crystallite size, k is the shape factor (0.9), λ = 0.154 nm, is the wavelength of the incident x-rays, β is the full width at half maxima (FHHM) in radian and θ is the scattering angle. The dislocation density. δ, which represents the length of the dislocation line per unit meter square, was enumerated using the following equation [13]:

$$\delta = \frac{1}{D^2}$$

The calculated values of crystallite size and the dislocation density (δ) using XRD data were enumerated in table-1. As visualized from the comparison of observed and JCPDS – values of 2θ (table-1), there is a shift in the peak positions towards left indicating changed lattice parameters.

To compute the lattice parameters using the most significant peak (222) the following relation were used [14]:

$$a^2 = [\frac{\lambda^2}{4sin^2\theta}](h^2 + k^2 + l^2)$$

where a is the lattice parameter and (hkl) are the Miller indices. The calculated value of lattice parameter using above relation was 10.27 Å which is higher than the standard value 10.12 Å (JCPDS-76-0152). The increase in lattice parameters represented the expansion in the crystal structure of the synthesized samples.

Table 1: Various calculated parameters for In_2O_3 nanostructures.

2θ (Observed)	2θ (JCPDS-76-0152)	FWHM(rad)	Crystallite size(nm)	Dislocation density, δ × 1015 m-2
21.021	21.490	0.00667	21.13	2.24
30.098	30.576	0.00675	21.25	2.21
34.952	35.591	0.00741	19.61	2.72
37.242	37.680	0.00873	16.76	3.56
41.266	41.833	0.00833	17.79	3.16
45.261	45.674	0.00789	19.04	2.76
50.511	51.007	0.00854	17.96	3.10
55.474	55.965	0.00744	21.06	2.25
58.544	59.113	0.00477	33.34	0.89
60.175	60.648	0.00925	17.31	3.34

The morphological analysis of the synthesized samples were carried out by using scanning electron microscope (SEM, HITACHI S-3600N, Japan) and the compositional analysis were precisely carried out by employing electron dispersive spectroscopy (EDX, Thermo Scientific, Ultra dry, Madison, WI 53711) coupled with SEM. Fig.3 shows the SEM images of the samples. The nanostructures were dense, uniformly distributed and nearly spherical in shape. Fig. 4 shows EDX of the synthesized samples taken at three different spots. The EDX depicted the presence of indium and oxygen only. No other element were found in the sample indicating the purity of the samples.

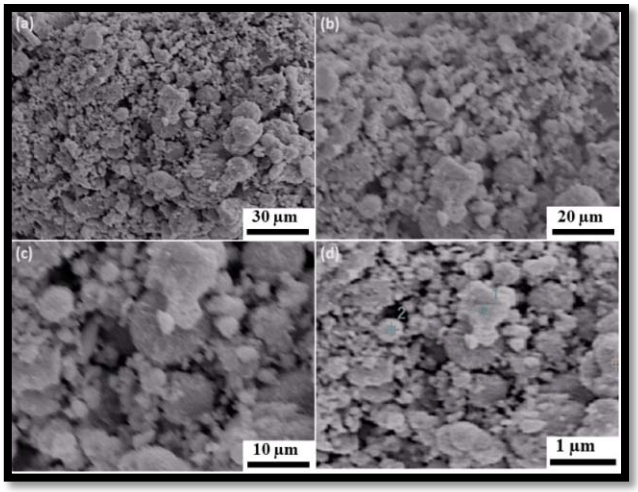

Figure 3. SEM images of In_2O_3 nanostructures

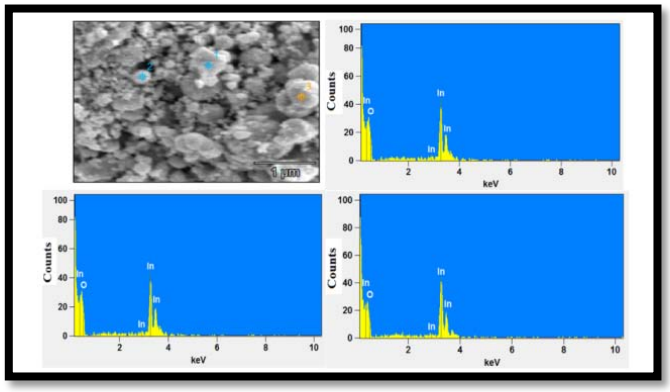

Figure 4. EDX of In_2O_3 nanostructures

3.1 Nucleation and growth

Nucleation is the fundamental process that involves the formation of solid phase and the creation of the ordered structures from other phases such as solid, liquid and gas. It is considered to be the first stage i.e. embryonic formation from the nuclei having dimensions in nanometer range which eventually grows in the form of final particles due to continuous aggregation and clustering of the molecules or ions [15-17]. In case of metal oxides, formation of hydrated hydroxides successively take part in condensation reactions. The formation of polymeric oxides by metal ions (olation process-condensation of M-OH_2 and HO-M groups) is followed by the oxolation process (condensation of 2 M-OH groups) which finally leads to the nucleation of a solid material [17, 18]. In homogeneous nucleation, the free energy change, ΔG, can be described by:

$$\mathbf{\Delta G = 4\pi r^2 \gamma - (4/3)\pi r^3 \Delta G_v}$$

where $\boldsymbol{A = 4\pi r^2}$, is the surface area, $\boldsymbol{\gamma}$, is the surface energy of the solid liquid interface and $\boldsymbol{\Delta G_v = RTln\frac{c_L}{c_S} = RT\,lnS}$, with $\boldsymbol{c_L}$ and $\boldsymbol{c_S}$ are the concentrations of the precursors in the liquid and solubility of the solid, respectively. For a stable nucleus to exist i.e. for minimum energy:

$$\mathbf{\frac{\partial}{\partial r}\Delta G = 0}$$

which corresponds to $\boldsymbol{r = \frac{2\gamma}{\Delta G_v}}$, referred to as critical radius of the nucleus represented as $\boldsymbol{r^*}$. The energy essential to form critical nucleus is:

$$\mathbf{\Delta G^* = {16\pi\gamma^3}/{3}\,(\Delta G_v)^2}$$

From above equation, it is obviously visible that for the formation of a nucleus, energy required is strongly reliant on surface energy and the supersaturation. The nucleation rate is given as, $\boldsymbol{N^* = N_0 \exp(-{\Delta G}/{kT})}$ which increases with the increase in supersaturation and decrease in surface energy [16]. After this embryonic stage i.e. nucleation, the growth take place up to the equilibration (determined by solubility) of precursor concentration with the metal oxide. The growth is kinetically limited, where growth rate is anticipated to be proportional to surface area of particle resulting in the faster growth of the larger particles but independent of particle size in case of pure polynuclear growth, if the unification of the surface atoms is slow. However, it is limited by the diffusion, where the growth rate has inverse radius dependence resulting in the faster growth of smaller particles as well as narrowing of size distribution, if the unification of atoms is fast [18]. In case of synthesis of metal oxide nanoparticles, the probable dominant growth is diffusion limited growth in comparison to kinetically limited growth. The nucleation and growth of nanoparticles of metal oxides generally leads to the formation of particles possessing spherical shape because of the fact that these structures possess the lowest surface energy which is in good agreement with surface energy theory. After these two important processes i.e. nucleation and growth, the process of aging starts by virtue of which the particle size changes. The aging occurs via Ostwald ripening and aggregation. The processes of aggregation, which depends on nanoparticle surface charge, pH of solution, and adsorbing molecular or ionic environment, takes place in a haphazard fashion or with a preference for epitaxial assembly reflecting that the experimental conditions strongly effect the process of aggregation.

4. CONCLUSION

In the present study, In_2O_3 nanoparticles having spherical shape were synthesized by a simple citrate gel process using indium nitrate, citric acid and de-ionized water as starting materials. The study focuses on the structural and morphology features of the In_2O_3 nanostructures. The x-ray diffraction (XRD) study revealed high phase purity and crystallinity with a crystallite size of 21.25 nm using the most significant peak

(222). Scanning electron microscopy revealed the formation of spherical nanostructures and electron dispersive spectroscopic (EDX) analysis confirmed presence of Indium and oxygen only. It would be interesting to analyze the effect of lower and the higher calcination temperature on the structure and morphology of the metal oxide nanoparticles synthesized by the citrate gel method.

5. ACKNOWLEDGEMENTS

The authors are highly thankful to NIT Srinagar The authors are also thankful to Material Science Division –IUAC, New Delhi) for providing experimental facilities.

REFERENCES

[1] A. Gurlo, M. Ivanovskaya, N. Barsan, M. Schweizer-Berberich, U. Weimar, W. Gopel, A. Dieguez, Grain size control in nanocrystalline In_2O_3 semiconductor gas sensors, Sens. Actuators B, Chem. 44 (1997) 327–333.

[2] Q.R. Zhao, Y. Gao, X. Bai, C.Z. Wu, Y. Xie, Facile synthesis of SnO_2 hollow nanospheres and applications in gas sensors and electrocatalysts, Eur. J. Inorg. Chem. (2006) 1643–1648.

[3] A. Murali, A. Barve, V.J. Leppert, S.H. Risbud, I.M. Kennedy, H.W. Lee, Synthesis and characterization of indium oxide nanoparticles, Nano Lett. 1 (2001) 287–289.

[4] D.H. Zhang, C. Li, S. Han, X.L. Liu, T. Tang, W. Jin, C.W. Zhou, Electronic transport studies of single-crystalline In_2O_3 nanowires, Appl. Phys. Lett. 82 (2003) 112–114.

[5] Xiaoqing Wang, Maofeng Zhang, Jinyun Liu, Tao Luo, Yitai Qian. Shape- and phase-controlled synthesis of In_2O_3 with various morphologies and their gas-sensing properties, *Sensors and Actuators B 137 (2009) 103–110.*

[6] C.Q.Wang, D.R. Chen, X.L. Jiao, C.L. Chen, Lotus-root-like In_2O_3 nanostructures: fabrication, characterization, and photoluminescence properties, J. Phys. Chem. C 111 (2007) 13398–13403.

[7] B.X. Li, Y. Xie, M. Jing, G.X. Rong, Y.C. Tang, G.Z. Zhang, In_2O_3 hollow microspheres: synthesis from designed $In(OH)_3$ precursors and applications in gas sensors and photocatalysis, Langmuir 22 (2006) 9380–9385.

[8] J. Yang, C.K. Lin, Z.L. Wang, J. Lin, $In(OH)_3$ and In_2O_3 nanorod bundles and spheres: microemulsion-mediated hydrothermal synthesis and luminescence properties, Inorg. Chem. 45 (2006) 8973–8979.

[9] Tahar R.B.H., T. Ban, Y. Ohya & Y. Takahashi, 1997. J. Appl. Phys. 82, 865.

[10] Yura K., K.C. Fredrikson & E. Matijevic, 1990. Coll. Surf. 50, 281.

[11] Hamada S., Y. Kudo & T. Kobayashi, 1993. Coll. Surf. A79, 227.

[12] Chen, H., Zhao, G., & Liu, Y. (2013). Low-temperature solution synthesis of CuO nanorods with thin diameter. *Materials letters*, *93*, 60-63.

[13] Siddiqui, H., Qureshi, M. S., & Haque, F. Z. (2014). One-step, template-free hydrothermal synthesis of CuO tetrapods. *Optik-International Journal for Light and Electron Optics*, *125*(17), 4663-4667.

[14] Al-Agel, F A et al 2014 A novel recipeto improve the magnetic properties of Mn doped CeO_2 as a room temperature ferromagnetic diluted metal oxide J. Mag. Magn. Mater. 36073–9

[15] De Yoreo, J. J. (2017). A holistic view of nucleation and self-assembly. *MRS Bulletin*, *42*(7), 525-536.

[16] Oskam, G. (2006). Metal oxide nanoparticles: synthesis, characterization and application. *Journal of Sol-Gel Science and Technology*, *37*(3), 161-164.

[17] Mehranpour, H., Askari, M., & Ghamsari, M. S. (2011). Nucleation and growth of TiO_2 nanoparticles. In *Nanomaterials*. InTech.

[18] Jolivet, J. P., Henry, M., & Livage, J. (2000). *Metal oxide chemistry and synthesis: from solution to solid state*. Wiley-Blackwell